Journal of Engineering and Applied Research (JEAR)

National University of Skills

Winter & Spring 2025, Vol. 2, No. 1, p.43-57

Journal Homepage: https://jear.tvu.ac.ir

doi: 10.48301/jear.2025.496526.1058

Design of a novel controller RIME-PID to improve the stability of a three-phase synchronous generator

Morteza Abdolhosseini [1], Rohollah Abdollahi [1*], Mohammad Hasan Eslami [1]

[1]Department of Electrical Engineering, Technical and Vocational University (TVU), Tehran, Iran

ARTICLE INFO

Article Type:
Original Research

Received: 12.30.2024
Revised: 02.03.2025
Accepted: 04.19.2025

Keyword:
Rotor angle
Three-phase synchronous generator
PID controller
RIME optimization algorithm

***Corresponding Author:**
Rohollah Abdollahi
Email: *abdollahi@tvu.ac.ir*

ABSTRACT

Significant disturbances in electrical power systems can destabilize operations, challenging the maintenance of synchronism among components. This paper introduces a novel three-phase synchronous generator rotor angle controller based on the RIME-PID algorithm, designed to mitigate rotor angle oscillations in transient and steady-state conditions while extending the generator's stable operating range. Existing methods in the literature often involve high computational loads, resulting in increased response times and reduced tracking speeds. In contrast, the proposed RIME-PID method, a physical approach to tuning PID controller parameters, adheres to power system stability criteria with lower computational demands and higher convergence speed. The RIME optimization algorithm optimizes PID controller coefficients across a wide search space, focusing on reducing settling time and overshoot. Linear state-space equations for a steam power plant are derived around the operating condition, and a 6th-order model based on Henkel's singular values is presented, incorporating a PID controller for rotor angle regulation. The stability of the proposed controller's output power is assessed using Bode and Nyquist criteria. Simulation results demonstrate that the RIME optimization algorithm outperforms fuzzy controllers, genetic algorithms, and Harris Hawks Optimization (HHO) in controlling the rotor angle of a three-phase synchronous generator. The RIME-PID controller achieves a rise time of 0.681 seconds, settling time of 8.8 seconds, peak time of 2.25 seconds, and an overshoot of 28.9%, significantly improved compared to other algorithms.

E-ISSN: 3060-6357

Introduction

Stability is a crucial aspect and necessity for dynamic systems [1; 2]. For instance, even though the turbine and generator protection system in a three-phase power plant is highly reliable, ensuring stability and minimizing disruptions in the power system is essential [3]. The rotor angle of the synchronous generator is a key parameter in maintaining stability in the generator of a three-phase power plant, determined by the angle disparity between the induction voltage in the stator winding and the generator's output voltage [4].

An excessive increase in the rotor angle leads to the departure of the generator from the range of stable operation and loss of synchronism, and an excessive decrease in the rotor angle also leads to a decrease in the active power delivered by the generator. The controller for the generator rotor angle plays a crucial role in restoring the generator to a stable operating state following any disturbances. As a result, researchers are consistently focused on devising effective control strategies for the generator rotor angle to ensure the stability of the power system and enhance the safety and efficiency of synchronous generators [5]. In [6], the detection of rotor position and the estimation of the rotor angle for a three-phase synchronous generator are suggested using an optical sensor. Additionally, another approach involves estimating the rotor angle by measuring power system parameters and utilizing a phase measurement unit, as outlined in [7] and [8]. Real-time rotor angle measurement using digital signal processing is presented in [9]. In the literature review, the PID controller is still used. In [10], the PID controller has been used to diagnose permanent magnet synchronous generator wind turbine and [11] to control the robot arm. To fine-tune the parameters of the PID controller, an improved arithmetic optimization algorithm is proposed in [12]. A modified structure of the tilt integral derivative (TID) controller is developed in [13] to control the rotor frequency of a power system. Existing controls in the literature review exhibit high settling time, rise time, overshoot, fluctuations, and computational load, resulting in increased response time and decreased tracking speed. In this paper, RIME-PID controller is used for the first time in the application of load angle control. The RIME-PID method is introduced as an innovative approach of essentially physical nature, aiming at fine-tuning the parameters that define the behavior of the PID controller. The method is designed in such a way that the stability requirements related to stable power systems are met, while simultaneously reducing the computational load and increasing the convergence speed. Furthermore, the RIME optimization algorithm performs a comprehensive exploration of the process involved in optimizing the coefficients of the PID controller over a wide range of space and uses two distinct strategies aimed at minimizing the settling time and reducing of overshoots during the system step response.

However, due to the high number of possible solutions in finding the optimal coefficients of the synchronous generator rotor angle PID controller, the use of metaheuristic algorithms is suggested. Based on meta-heuristic algorithms, a rotor angle controller based on GA-PID in [14] and a rotor angle controller based on HHO-PID in [15] have been used to improve the performance stability of the synchronous generator of the power plant. However, it can be seen that the rise time, settling time, and overshoot in the GA-PID algorithm are too high and are not acceptable compared to the transient fluctuations of the power system. Also, the HHO-PID algorithm has a large computational rotor, which leads to an increase in response time and a decrease in tracking speed. In [16], to increase the rotor angle stability of power systems, the marine predator algorithm based on PID cascade control is used. The study outlines the utilization of the power system stabilizer for rotor angle control in the synchronous generator [17]. Results from [16; 17] indicate that the controlled rotor angle experiences notable fluctuations and extended settling time. Advanced DC-Link voltage regulation via sliding mode control is provided for generator systems using three-phase inverters in [18]. In [19], a multi-objective control scheme is proposed for a battery energy storage system as a grid-independent distributed energy source in a synchronous generator. Using a fractional order PI controller, an analytical study of load variations on the terminal voltage and frequency of a three-phase synchronous generator is presented in [20]. The implementation of automatic detection, identification and quantification of vehicles through artificial intelligence in the field of transportation management is described in [21; 22].
Hence, with this approach, this paper reduces a complete steam power plant model using Hankel singular values to a 6th order model and proposes a novel synchronous generator rotor angle controller based on the RIME-PID algorithm, with two strategies to minimize settling time and overshoot, in order to meet the power system stability requirements. The organization of the paper is as follows: in the second section, the transfer function of the steam power plant is mentioned, and in the third section, the RIME algorithm is introduced. In the fourth and fifth sections, the simulation results and conclusions are presented, respectively.

Transfer function of steam power plant

The structure of the steam power plant along with the proposed generator rotor angle controller based on the RIME optimization algorithm is shown in Figure 1. It should be noted that the equivalent circuit parameters of the steam power plant used for simulation are also presented in this figure. In this section, the comprehensive transfer function of the steam power plant is first presented, then with the approach of reducing the computational rotor, based on Hankel's singular values, this 14-variable comprehensive model is approximated to the 6th order model.

In this paper, for transient dynamic studies, a 14-variable non-linear model of the steam power plant is presented based on the contrast between the electrical torque T_e and the mechanical torque T_m (shown in equation (1)).

$$T_e = \psi_d I_q - \psi_q I_d$$
$$T_m = F_{HP}Y_{HP} + F_{IP}Y_{IP} + F_{LP}Y_{LP} \quad (1)$$

Based on the transfer function shown in Figure 1, the state variables, the state vector, and the input vector of the 14-variable non-linear model of the steam power plant are expressed as follows:

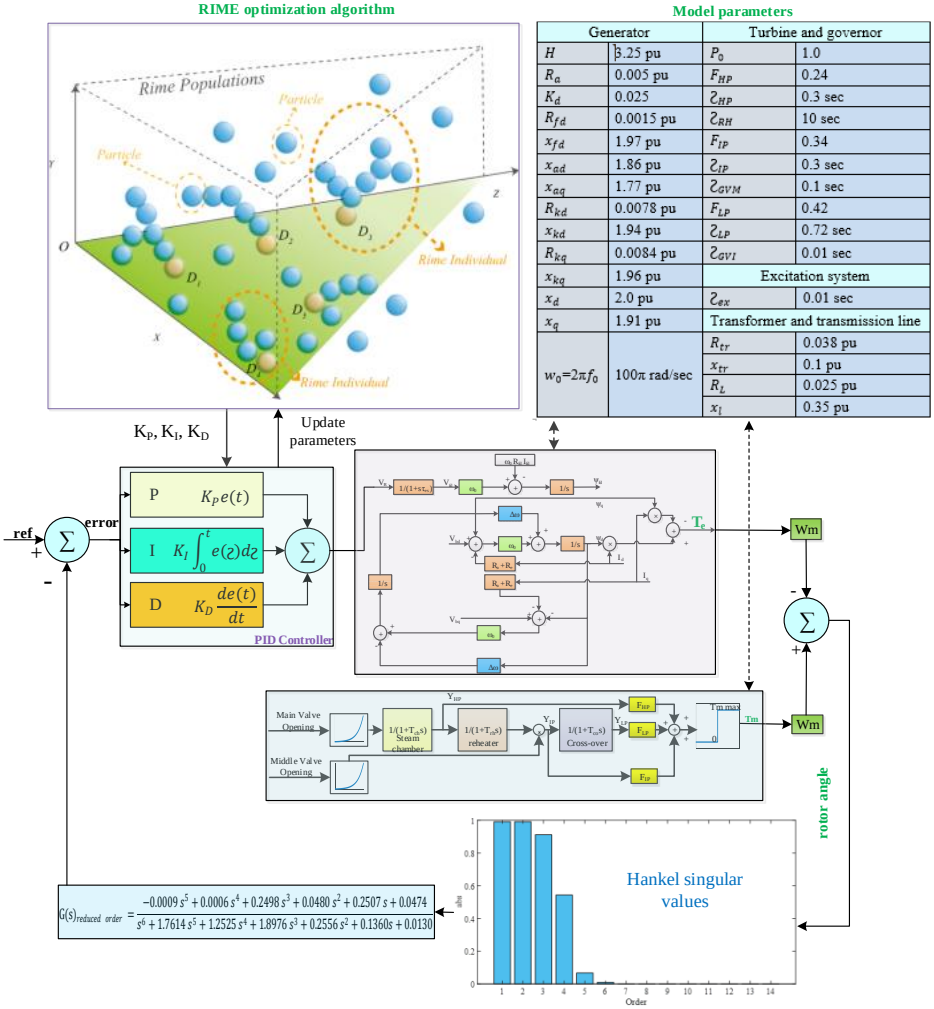

Generator		Turbine and governor	
H	3.25 pu	P_0	1.0
R_a	0.005 pu	F_{HP}	0.24
K_d	0.025	τ_{HP}	0.3 sec
R_{fd}	0.0015 pu	τ_{RH}	10 sec
x_{fd}	1.97 pu	F_{IP}	0.34
x_{ad}	1.86 pu	τ_{IP}	0.3 sec
x_{aq}	1.77 pu	τ_{GVM}	0.1 sec
R_{kd}	0.0078 pu	F_{LP}	0.42
x_{kd}	1.94 pu	τ_{LP}	0.72 sec
R_{kq}	0.0084 pu	τ_{GVI}	0.01 sec
x_{kq}	1.96 pu	Excitation system	
x_d	2.0 pu	τ_{ex}	0.01 sec
x_q	1.91 pu	Transformer and transmission line	
$w_0=2\pi f_0$	100π rad/sec	R_{tr}	0.038 pu
		x_{tr}	0.1 pu
		R_L	0.025 pu
		x_l	0.35 pu

$$G(s)_{reduced\ order} = \frac{-0.0009\,s^5 + 0.0006\,s^4 + 0.2498\,s^3 + 0.0480\,s^2 + 0.2507\,s + 0.0474}{s^6 + 1.7614\,s^5 + 1.2525\,s^4 + 1.8976\,s^3 + 0.2556\,s^2 + 0.1360s + 0.0130}$$

Figure 1. The structure of the steam power plant along with the proposed RIME-PID rotor angle controller

$$X = [\delta, \Delta\omega, \psi_{fd}, \psi_d, \psi_{kd}, \psi_q, \psi_{kq}, V_{fd}, Y_{HP}, Y_{RH}, Y_{IP}, Y_{LP}, G_{VM}, G_{VI}] \quad (2)$$

$$\mathrm{U} = (U_g V_R)^T \quad \text{و} \quad U_g = U_{GM} = U_{GI} \tag{3}$$

$$\begin{aligned}
\dot{x}_1 &= x_2 \\
\dot{x}_2 &= w_0(F_{HP}x_9 + F_{IP}x_{11} + F_{LP}x_{12} - x_6(y_{1d}x_4 + y_{4d}x_3 + y_{5d}x_5) + \\
&\quad x_4\big(y_{1q}x_6 + y_{3q}x_7\big) - K_d x_2/2H \\
\dot{x}_3 &= w_0(x_8 - R_{fd}(y_{4d}x_4 + y_{2d}x_3 + y_{6d}x_5)) \\
\dot{x}_4 &= w_0\big(V_b sinx_1 + x_6 - (R_a + R_e)(y_{1d}x_4 + y_{4d}x_3 + y_{5d}x_5)\big) + x_2 x_6 \\
\dot{x}_5 &= -w_0 R_{kd}(y_{5d}x_4 + y_{6d}x_3 + y_{3d}x_5) \\
\dot{x}_6 &= w_0\left(V_b cosx_1 - x_4 - (R_a + R_e)\big(y_{1q}x_6 + y_{3q}x_7\big)\right) - x_2 x_3 \\
\dot{x}_7 &= -w_0 R_{kq}\big(y_{3q}x_6 + y_{2q}x_7\big) \\
\dot{x}_8 &= (u_2 - x_8)/\mathcal{Z}_{ex} \\
\dot{x}_9 &= (P_0 x_{13} - x_9)/\mathcal{Z}_{HP} \\
\dot{x}_{10} &= (x_9 - x_{10})/\mathcal{Z}_{RH} \\
\dot{x}_{11} &= (x_{10}x_{14} - x_{11})/\mathcal{Z}_{IP} \\
\dot{x}_{12} &= (x_{11} - x_{12})/\mathcal{Z}_{LP} \\
\dot{x}_{13} &= (u_1 - x_{13})/\mathcal{Z}_{GVM} \\
\dot{x}_{14} &= (u_1 - x_{14})/\mathcal{Z}_{GVI}
\end{aligned} \tag{4}$$

By linearizing the 14-variable non-linear model of the steam power plant around the operating point, the transfer function of the steam power plant is obtained as equation (5):

$$\begin{aligned}
G(s) = {} & (19.41s^{10} + 2372\,s^9 + 4.513e04s^8 + 2.07\,e05\,s^7 + 3.301e05s^6 + \\
& 2.666e05s^5 + 2.882e05s^4 + 6.198e04s^3 + 3177s^2 + 37.2s + 0.06977)/ \\
& (s^{14} + 218.2\,s^{13} + 1.375e04s^{12} + 2.036e05\,s^{11} + 1.103e06\,s^{10} + \\
& 2.624e06\,s^9 + 3.106e06\,s^8 + 2.889e06\,s^7 + 2.178e06\,s^6 + 4.897e05\,s^5 + \\
& 1.62e05\,s^4 + 2.144e04\,s^3 + 923.4\,s^2 + 10.29\,s + 0.01911)
\end{aligned} \tag{5}$$

As seen in equation 5, the implementation of the controller for this 14th-order system has high complexity [14]. Therefore, to design the controller structure more simply, the approximation of the reduced order model has been done by cutting the modes in a coprime factorization in the full order model [16]. In this method, singular Hankel values are calculated, which represent the relative energy contribution of each state in simultaneous factorization. This method is related to the feedback-balanced cut method, but it can be used to reduce the controller order. Using Hankel's singular value method, the 6-order linear model of the steam power plant to implement the proposed controller is shown in equation 6.

$$\mathrm{G(s)}_{reduced\ order} = \frac{-0.0009\,s^5 + 0.0006\,s^4 + 0.2498\,s^3 + 0.0480\,s^2 + 0.2507\,s + 0.0474}{s^6 + 1.7614\,s^5 + 1.2525\,s^4 + 1.8976\,s^3 + 0.2556\,s^2 + 0.1360s + 0.0130} \tag{6}$$

RIME optimization algorithm

The RIME optimization algorithm's overall framework is illustrated in Figure 2. RIME ice refers to the non-dense vapor in the air that freezes at low temperatures. Environmental influences cause the RIME ice to grow until it reaches a relatively stable state and then ceases. The development of RIME involves two categories: soft RIME and hard RIME. Soft RIME exists in a wind environment with low wind speed, with varying directions simultaneously, randomly, and in a plane of height. On the other hand, hard RIME occurs in the environment with high wind speed (gust), almost in a certain direction and height. In fact, the RIME optimization method is able to quickly check the entire search space in the initial iteration so that this algorithm does not end up in the local optimum. This optimization algorithm has four stages: initialization, soft search, hard drilling, and greedy selection.

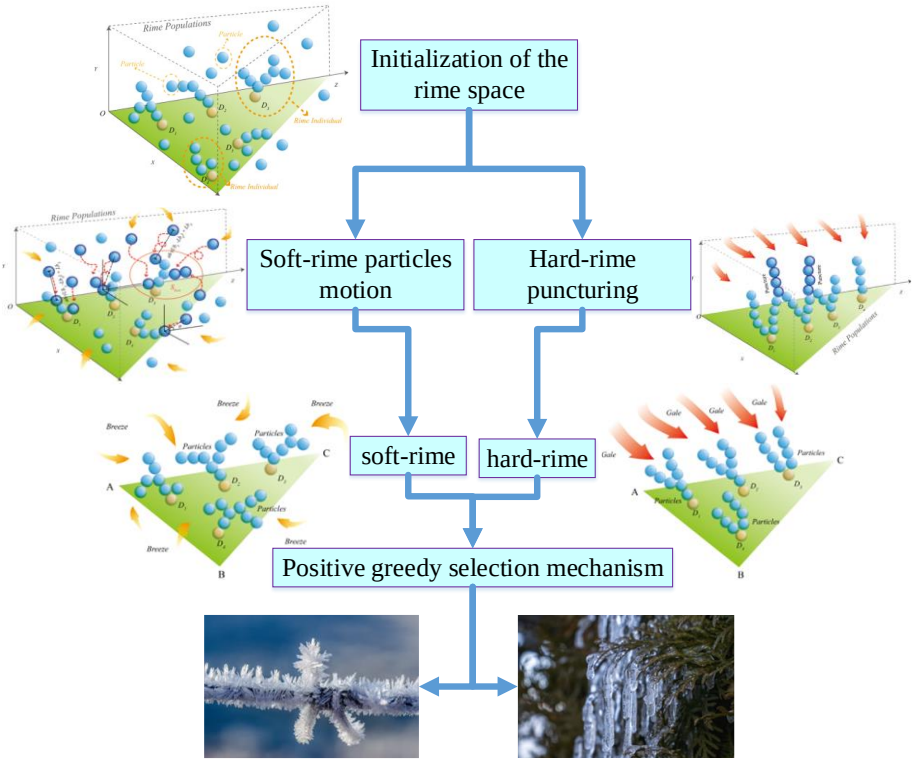

Figure 2. Structure of RIME optimization algorithm

Initially, the entire population R of RIME is initialized. As shown in equation (7), the population R can be represented by xij particles, where i is the ordinal number of the RIME agent and j is the ordinal number of the RIME particle.

$$R = \begin{bmatrix} x_{11} & x_{12} & \cdots & x_{1j} \\ x_{21} & x_{22} & \cdots & x_{2j} \\ \vdots & \vdots & \ddots & \vdots \\ x_{i1} & x_{i2} & \cdots & x_{ij} \end{bmatrix} \quad (7)$$

soft search Condensation of RIME particles leading to soft agents has the following results:

• Each xij particle is wandering under the influence of environmental conditions before condensation.

• The stability of soft RIME can be influenced by the combination of free space particles with compacted particles.

• Variations in the degree of particle density result in differences in the distance between the centers of two connected particles.

• If the particle does not move within the range of the particle escape slogan, there is no compression between these two particles.

• RIME growth is soft, limited and continues until stable conditions are reached.

According to the mentioned feature, the new position of RIME particles is shown in equation (8).

$$R_{ij}^{new} = R_{best,j} + r_1 \cdot \left[\!\left[\cos\right]\!\right] \pi \cdot \frac{t}{10 \cdot T}\Big) \cdot \left(1 - \frac{\left[\frac{5t}{T}\right]}{5}\right) \cdot \left(h \cdot \left(Ub_{ij} - Lb_{ij}\right) + Lb_{ij}\right) \quad (8)$$

where, R_{ij}^{new} is the updated position of the particle, i and j represent the j th particle of the i th rime agent. $R_{best,j}$, j is the best RIME agent in population R. The parameter r_1 is a random number less than one and controls the direction of movement of the particles. h is the adhesion strength, which is a positive random number less than one. t and T are the current iteration number and the maximum iteration number of the algorithm, respectively, which is the correct part of 5t/T in the considered relationship. Ub_{ij} and Lb_{ij} are the upper and lower limits of the effective search space, respectively.

hard drilling

In strong wind conditions, due to the same direction of growth, a phenomenon called RIME hole is created. Using the punching mechanism can be used to update agents. Therefore, hard drilling will lead to convergence, not getting stuck in the

local optimum and ultimately increase the accuracy of the algorithm. The phenomenon of perforation is shown in equation (9).

$$R_{ij}^{new} = R_{best,j} \tag{9}$$

where R_{ij}^{new} is the updated new position of the particle and $R_{best,j}$, the jth particle is the best RIME agent in population R.

greedy choice

In the RIME algorithm, in order to improve the population, the value of the new factor is compared with the value of the factor of the previous stage, and if the value of the new factor is better than the value of the previous factor, it will be replaced. In greedy selection, factors with bad value are generally eliminated, which will lead to increased response speed and improved optimization operations.

Simulation results

The flowchart in Figure 3 illustrates the RIME-PID algorithm, which is designed to manage the rotor angle of the synchronous generator. This algorithm takes into consideration two approaches aimed at reducing the settling time and minimizing the overshoot of the step response. At first, the complete fourteenth-degree model of the system (steam power plant) is defined and the working point of the system is determined by considering the active power of 1 pu, the reactive power of 0.5 pu, and the infinite bus voltage of 1.05 pu. Following this process, the values of the state variables and system inputs are established based on the system's operating point. The 6th-order linear model is then derived using these state variables. Notably, the rotor angle is the resultant output of the linearized model transfer function. Ultimately, the PID controller's optimal coefficients are fine-tuned using the RIME optimization algorithm, which considers both the approaches of decreasing the settling time and minimizing the overshoot in the step response.

$$Z = w_1 \times OS + w_2 \times ST + w_3 \times RT + w_4 \times SI \tag{10}$$

where coefficients of the objective function are denoted as w_1 to w_4, while OS represents the overshoot, ST represents the settling time, and RT represents the rising time. The stability index, SI, is defined by equation (11), and T represents the closed-loop transfer function.

$$SI = \frac{-1}{\min[\max[real\big(pole(T)\big)],0]} \tag{11}$$

The stability of the system is contingent upon the real part of all the roots of the closed loop transfer function being less than zero. In order to configure the RIME algorithm parameters, the upper limits for the K_I, K_P, and K_D coefficients of the PID controller are established as [30, 1, and 10] respectively, while the lower limits for these coefficients are defined as [1.01, 0.01 and 1.01] respectively. Also, the number of decision variables is equal to 3, and the number of 50 repetitions is considered.

In this paper, the proposed RIME algorithm adjusts the coefficients of the PID controller to stabilize the rotor angle of the synchronous generator, taking into account the two approaches of overshoot reduction (I) and the settling time reduction approach (II). In approach, I, considering the weights of the objective function w_1, w_2, w_3, and w_4, respectively, 0.2, 0.6, 0.1, and 0.1, the coefficients K_I, K_P and K_D of the PID controller are 1.01, 0.1143, and 6.3321. are calculated. Also, in approach II, considering the weights of w_1, w_2, w_3, and w_4 as 0.6, 0.2, 0.1, and 0.1 respectively, the coefficients K_I, K_P, and K_D of the PID controller are 1.01, 1, and 14.9696 respectively. are calculated.

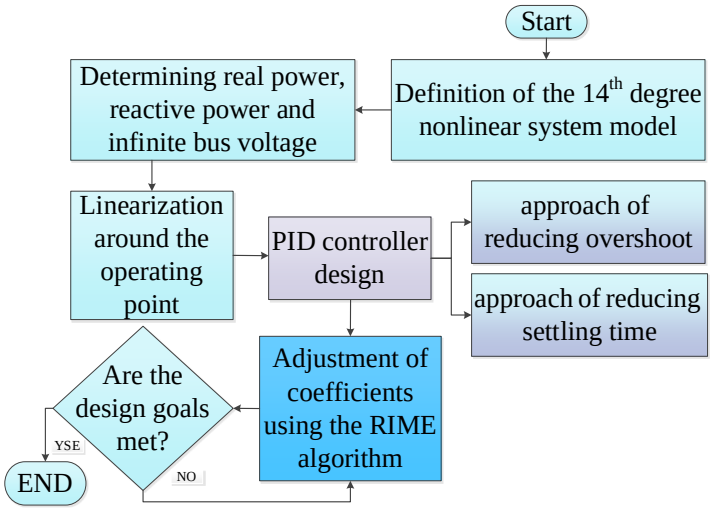

Figure 3. Flowchart of the proposed RIME-PID algorithm

An assessment of the stability of the RIME-PID controller was conducted by plotting the Nyquist diagram and Bode diagram for the rotor angle, as illustrated in Figures 4 and 5. As can be seen in Figure 4, since the open loop transfer function of the system in both approaches of overshoot reduction (I) and settling time reduction (II) does not have an instability pole and also does not bypass the Nyquist diagram -1 point, therefore The system rotor angle output is stable. According to Figure 5, the gain margin in approach I is 0.9708 and in approach II is 2.1740, as well as the phase margin in approach I is 1.1247 and in approach II

is 23.8386. The gain margin and phase margin values are both positive, indicating that the RIME-PID controller will ensure the stability of the rotor angle.

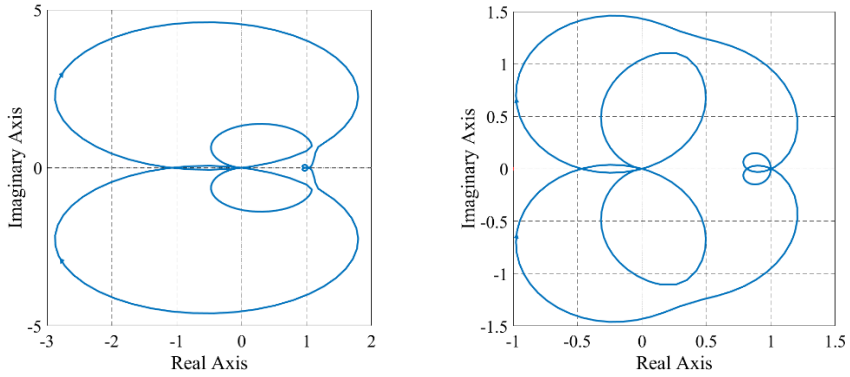

(a) (b)

Figure 4. Nyquist diagram of the rotor angle (a) approach to reduce the settling time (I), (b) approach to reduce the overshoot (II)

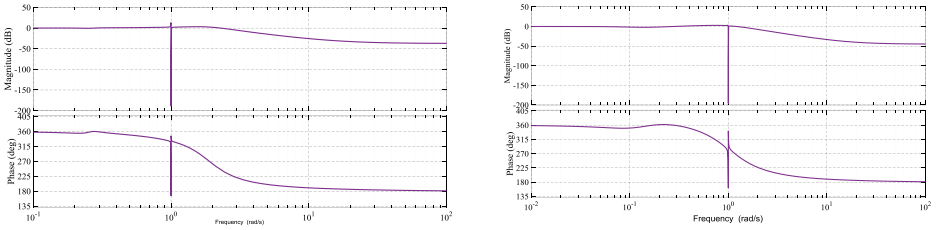

(a) (b)

Figure 5. Diagram of rotor angle. (a) approach to reduce the overshoot (II), (b) approach to reduce the settling time (I)

The characteristic of the rotor angle of the PID controller of the synchronous generator without and using the RIME algorithm is obtained by applying the unit step as the input Ug to the system according to Figure 6. As can be seen in this figure, the characteristic of the rotor angle without using the RIME algorithm is very fluctuating and has a high and unfavorable overshoot and settling time (3000 seconds). If the rotor angle PID controller using the RIME-PID algorithm under both approaches shows a good performance in the stable rotor angle of the synchronous generator.

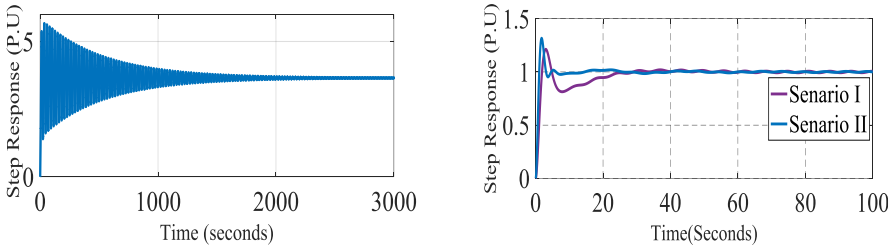

(a) (b)

Figure 6. PID controller rotor angle characteristic for step input. (a) without using the RIME algorithm, (b) using the RIME algorithm

The relationship between the output power of the synchronous generator and the rotor angle is expressed as follows [8].

$$P = P_{max} \sin \delta \tag{12}$$

As stated earlier, the purpose of presenting the RIME-PID-based rotor angle controller in this paper is to maintain the stability of the three-phase synchronous generator in critical (sudden and severe) active power fluctuations. Figure 7 shows the output power of the synchronous generator under the rotor angle PID controller, without and using the RIME algorithm. As can be seen in Figure 7(a), the synchronous generator without a RIME-PID controller is not able to respond to critical fluctuations and the output power becomes fluctuating and unstable. Therefore, with the installation of the RIME-PID rotor angle controller, the three-phase synchronous generator of the power plant can respond and mitigate the strong fluctuations of the active power and stabilize the power system in less than 10 seconds

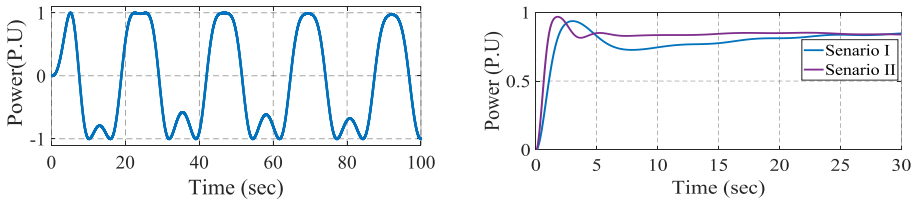

(a) (b)

Figure 7. Output power of the synchronous generator. (a) without using the RIME algorithm, (b) using the RIME algorithm

To highlight the contribution of the proposed rotor angle controller, a comparison has been made between the proposed RIME-PID controller and other existing rotor angle controllers. The results of this comparison, which include settling time, peak time, overshoot rate, and rise time of the step response, are listed in Figure 8. As can be seen in this Figure, in terms of rise time, settling time,

and peak time, the RIME-PID controller has a better performance compared to other existing algorithms. Although overshooting in the RIME algorithm with approach II is high and equal to 62.5%, it should be noted that in approach I, this time has been reduced to 28.9% by the proposed algorithm, which is the lowest percentage of overshooting compared to other algorithms. In addition, the step response characteristics of the RIME algorithm have been improved more properly compared to the two HHO and AOA algorithms, which leads to an increase in the efficiency of the PID controller in critical conditions and transition times.

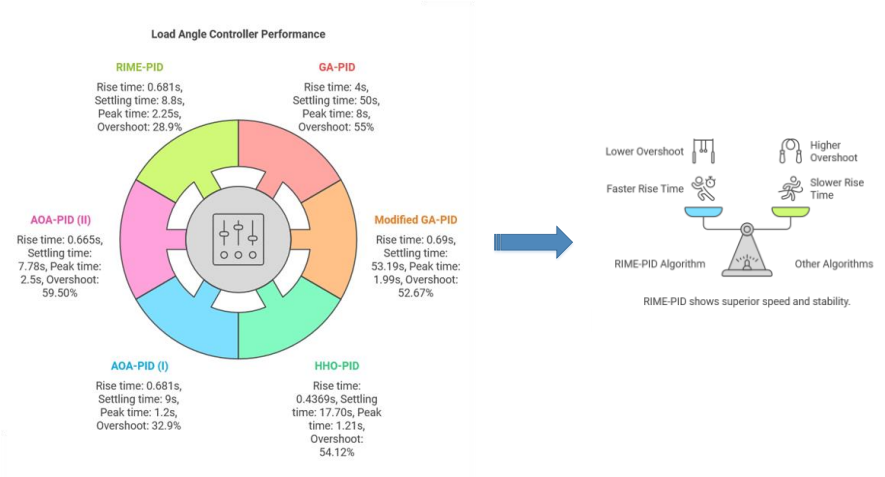

Figure 8. Compares the performance of the rotor angle controller based on the proposed RIME-PID algorithm with other existing algorithms

Conclusion

In this paper, a rotor angle controller based on RIME-PID is presented to maintain the stability of a three-phase synchronous generator in critical fluctuations of active power. The RIME algorithm, as suggested, modifies the PID controller's coefficients to stabilize the rotor angle of the synchronous generator. This is achieved by taking into account two different strategies: overshoot reduction and settling time reduction. The RIME algorithm performs optimization processes of PID controller coefficients in a wide range of search spaces by using a soft search strategy, hard drilling mechanism, and positive greedy selection mechanism. The stability of the proposed RIME-PID rotor angle controller is confirmed by Nyquist and Bode diagrams. Also, to highlight the contribution of the proposed rotor angle controller, a comparison has been made between the proposed RIME-PID controller and other available rotor angle controllers. The resultts validate the superior effectiveness of the newly introduced RIME-PID controller in diminishing rise time, settling time, peak time,

and the level of step response overshoot when juxtaposed with alternative algorithms. Overall, it can be inferred that the suggested RIME-PID controller exhibits the most optimal performance in regulating the rotor angle of the synchronous generator and ensuring the stability of the power system.

References

[1] Abdolhosseini, M., Abdollahi, R., & Rajaee, M. (2021). Designing of PIλDδ controller for PMBLDC motor using metaheuristic algorithms. *Karafan Journal*, *17*(4), 149–165. https://doi.org/10.48301/kssa.2021.128401

[2] Mofidian, R., Hassankhani, I., Jahanshahi, M., Hosseini, S. S., & Miansari, M. (2024). Cost Effective Design of a 200 kW On-grid Rooftop Photovoltaic System Using PVsyst Software in Shiraz. *Journal of Engineering and Applied Research*, *1*(1), 13–24. https://doi.org/10.48301/jear.2024.194109

[3] Karrari, M. (2015). *power systems dynamics and control*. Amir Kabir University Publishing, Iran. https://www.amazon.com/Power-System-Dynamics-Control-Engineering/dp/0817646736

[4] Korram, S., & Ezadfar, H. R. . (2015). *A method for calculating accurate the reference value of synchronous generator rotor angle* The National Conference of New Idea on Electrical Engineering, Esfahan, Iran. https://civilica.com/doc/533689/

[5] Kundur, P. (1994). *Power System Stability and Control*. McGraw-Hill, USA. https://www.amazon.com/Power-System-Stability-Control-Second/dp/1260473546

[6] Sumina, D., Sala, A., & Malaric, R. (2010). Determination of load angle for salient-pole synchronous machine. *Measurement science review*, *10*(3), 89. https://doi.org/10.2478/v10048-010-0018-2

[7] Čuček, H., Sumina, D., & Švigir, N. (2010). *Synchronous generator load angle estimation* Melecon 2010-2010 15th IEEE Mediterranean Electrotechnical Conference, https://ieeexplore.ieee.org/document/5476348

[8] Aghamohammadi, M. R., Kazemi, E., & shivaei, M. . (2013). *Provide a method for estimating the rotor angle of a synchronous generator using parameters that can be measured with PMU* International Conference on Electricity, Power Research Institute, Tehran, Iran. https://elmnet.ir/vslgg?id=20770807-31891

[9] Hosseini, S. M., Abdollahi, R., & Karrari, M. (2018). Inclusive design and implementation of online load angle measurement for real-time transient stability improvement of a synchronous generator in a smart grid. *IEEE Transactions on Industrial Electronics*, *65*(11), 8966–8972. https://doi.org/10.1109/TIE.2018.2811394

[10] Khodakaramzadeh, S., Ayati, M., & Haeri Yazdi, M. (2020). Fault diagnosis of a permanent magnet synchronous generator wind turbine. *Journal of Electrical and Computer Engineering Innovations (JECEI)*, *9*(2), 143–152. https://doi.org/10.22061/jecei.2020.7424.408

[11] Jamshidi, F., & Vaghefi, M. (2018). WOA-based interval type II fuzzy fractional-order controller design for a two-link robot arm. *Journal of Electrical and Computer Engineering Innovations (JECEI)*, *7*(1), 69–82. https://doi.org/10.22061/jecei.2019.5783.256

[12] Izci, D., Ekinci, S., Kayri, M., & Eker, E. (2022). A novel improved arithmetic optimization algorithm for optimal design of PID controlled and Bode's ideal transfer function based automobile cruise control system. *Evolving Systems*, *13*(3), 453–468. https://doi.org/10.1007/s12530-021-09402-4

[13] Ahmed, M., Magdy, G., Khamies, M., & Kamel, S. (2022). Modified TID controller for load frequency control of a two-area interconnected diverse-unit power system. *International Journal of Electrical Power & Energy Systems*, *135*, 107528. https://doi.org/10.1016/j.ijepes.2021.107528

[14] Korram, S., & Ezadfar, H. R. . (2016). *Use of genetic algorithm in optimal control of real power and rotor angle of synchronous generator* International conference on recent trends in engineering and materials science, Dubai, UAE. https://civilica.com/doc/482221/

[15] Abdolhosseini, M., & Abdollahi, R. (2022). Design of HHO-PID Controllers for Load Angle of Power Plant Synchronous Generators. *International Transactions on Electrical Energy Systems*, *2022*(1), 7746062. https://doi.org/10.1155/2022/7746062

[16] Yakout, A., Sabry, W., & Hasanien, H. M. (2021). Enhancing rotor angle stability of power systems using marine predator algorithm based cascaded PID control. *Ain Shams Engineering Journal*, *12*(2), 1849–1857. https://doi.org/10.1016/j.asej.2020.10.018

[17] Abdollahi, R. (2023). Modeling by order reducing the load angle of a three-phase synchronous generator and designing an AOA-PID controller to control the load angle. *Journal of Modeling in Engineering*, *21*, 83–99. https://doi.org/10.22075/jme.2023.27635.2296

[18] Rahman, M. L., & Shatil, M. A. H. (2021). *Design and implementation of a synchronous generator with rotor angle stability control for damping interarea oscillations of interconnected power systems via PSS* 2021 International Conference on Information and Communication Technology for Sustainable Development (ICICT4SD), https://doi.org/10.1109/ICICT4SD50815.2021.9396810

[19] Zhao, M., Zhang, S., Zhang, C., Li, X., & Dong, Y. (2025). Improved DC-link voltage sliding mode control for permanent magnet synchronous generator systems with three-phase AC-DC converters. *IEEE Journal of Emerging and Selected Topics in Power Electronics*. https://doi.org/10.1109/JESTPE.2025.3529183

[20] Ghafouri, S., Gharehpetian, G. B., Naderi, M. S., & Mahdavi, M. S. (2024). An integrated multi-function control scheme for independent BESS in islanded synchronous generator-based microgrids. *IEEE Transactions on Industrial Informatics*. https://doi.org/10.1109/TII.2024.3435357

[21] Panigrahi, D. (2025). Analytical Studies of Load Variation on Terminal Voltage and Frequency of Three Phase Synchronous Generator Using Fractional Order PI Controller. In *In Computing, Communication and Intelligence*. CRC Press. https://www.taylorfrancis.com/chapters/edit/10.1201/9781003581215-17/analytical-studies-load-variation-terminal-voltage-frequency-three-phase-synchronous-generator-using-fractional-order-pi-controller-dheeman-panigrahi

[22] Akoushideh, A., Sadat, S. S., & Shahbahrami, A. (2024). Detecting, identifying, and counting vehicles based on deep learning algorithms in video surveillance

systems. *Journal of Engineering and Applied Research*, *1*(2), 79–90. https://doi.org/10.48301/jear.2024.459050.1027